EnvironmentAsia
The international journal by the Thai Society of Higher Education Institutes on Environment
EnvironmentAsia 18(1) 2025 93-109
DOI 10.14456/ea.2025.8
ISSN 1906-1714; ONLINE ISSN: 2586-8861

Polystyrene Nanoplastic-Induced Toxicity in Neuronal Cells

Ming Hui Wong[1], Rhun Yian Koh[2], Boon Keat Tan[3], Yong Qi Leong[4], and Chooi Ling Lim[2*]

[1]Warwick Medical School, University of Warwick, Coventry CV4 7AL, United Kingdom
[2]Division of Applied Biomedical Science and Biotechnology, School of Health Sciences, IMU University, 126 Jalil Perkasa 19, Bukit Jalil, 57000 Kuala Lumpur, Malaysia
[3]Division of Human Biology, School of Medicine, IMU University, 126 Jalil Perkasa 19, Bukit Jalil, 57000 Kuala Lumpur, Malaysia
[4]School of Pharmacy, Monash University Malaysia, Jalan Lagoon Selatan, 47500 Bandar Sunway, Selangor, Malaysia.

*Corresponding author: chooi_linglim@imu.edu.my
Received: May 8, 2024; Revised: September 4, 2024; Accepted: October 11, 2024

Abstract

Plastic pollution is a decades-long environmental challenge, contaminating food, water, and even breathable air. Evidence on the permeability of small, fragmented plastic particles called nanoplastics through the animal blood brain barrier invoked concerns of potential neurotoxicity in humans. Thus, this study investigated the mechanism of nanoplastic-induced toxicity in a neuronal cell-line. Polystyrene was utilised due to their ubiquity as a plastic pollutant and the second most common plastic type found in human blood. SH-SY5Y neuroblastoma cells were exposed to variable concentrations (0.2% to 0.0000128%) and sizes (20 - 100 nm) of polystyrene nanoplastics (PS-NPs). Fluorescence microscopy findings suggest that PS-NPs were engulfed by SH-SY5Y cells. PS-NP effect on cell viability was dependent on the concentration and size of PS-NPs. Increased PS-NP concentrations (from 0.008%) reduced cell viability, whereby the smallest particle sizes inflicted the strongest cytotoxicity (IC_{50} of 20 nm PS-NPs = 0.0055%) ($p < 0.05$). Increased intracellular ROS levels were also found in the treated cells compared to the control. Hoechst 33258 staining and flow cytometry suggested apoptotic induction by 18.18% in 24 hours. In conclusion, PS-NPs showed accumulation and induced apoptosis in SH-SY5Y cells, suggesting potential neurotoxicity upon human exposure to nanoplastics.

Keywords: Polystyrene nanoplastics; SH-SY5Y neuroblastoma cell line; Cytotoxicity; Apoptosis; Reactive oxygen species (ROS)

1. Introduction

Global data has projected an alarming increase of plastic wastes from 2 million tons in 1950 to more than 400 million tons in just over half a century later. In the year 2019, the number of plastics cumulated worldwide would reach over one tonne for every living person (Ritchie and Roser, 2018). Furthermore, with the COVID 19 pandemic, these figures are expected to increase due to the tremendous production of one-use plastic objects in both daily consumption and medical supplies like gloves, face shields, masks, and other personal protective equipment (PPE) (Windheim *et al.,* 2022). Synthetic fibres such as polyester, acrylic and nylon are a form of plastic, and are said to make up almost 60%

of our garments (Savelli, 2019) resulting in around 0.5 million tonnes of microplastics released into the ocean annually just from doing laundry (Lai *et al.,* 2022).

Plastic polymers can be categorised based on the sizes of their particles. Plastics more than 5 mm are recognised as macroplastics (MaPs). Due to natural weathering conditions (such as rain and sunshine) and frictional abrasions by wind and waves, these MaPs are further reduced to microplastics (MPs) (less than 5 mm) and nanoplastics (NPs) (less than 1 μm) (Gigault *et al.,* 2018). Once in this form, the particles persist for a long period of time given their high resistance to biodegradation. Although polystyrene (PS) took only three weeks of UV exposure to be reduced to a nano-ranged particle size (Lambert and Wagner, 2016), it takes 500 years for styrofoam to biodegrade in nature (Joseph, 2019). This means that plastics are able to persist in their micro or nanoform in the environment for an extremely long time, posing a huge threat to the global health of nature and its living inhabitants.

Following the discovery of microplastic toxicity in various animal studies, the light of scientific interest has slowly shifted to nanoplastics, as in theory, due to their smaller size and greater abundance, they have a higher potential of permeability through biological barriers and would cause more morbidity (Sharma *et al.,* 2022). Leslie *et al.* (2022), discovered that the three most abundant type of plastic quantified in human blood were polypropylene, polystyrene, and polyethylene. Notably, these polymers are also frequently used for food or beverage packaging and other items encountered by humans on a daily basis. It has been found that the three possible routes of plastic intake into the human body are by inhalation, absorption and ingestion (Abbasi, 2021). Regarding the route of inhalation, microplastics were discovered in inhaled air by micro-Roman imaging spectroscopy (Geng *et al.,* 2023). The discovery of plastic particles in lung tissues also dates to even the 1990s, where plastic fibres were obtained from patients undergoing lung resection surgery (Pauly *et al.,* 1998). Regarding topical absorption, scientists believe that it is through compromised skin due to injury or disease that increases the permeability of nanoplastics into the skin barrier, resulting in unintended absorption of plastic particles from the external environment into the human body (Lett *et al.,* 2021). Regarding oral ingestion, large scale quantification efforts have yielded evidence of microplastics and nanoplastics in common food products and beverages. A study by WWF (Mason, 2019) revealed that humans ingest about 5 g of plastic a week, indicating the extent of plastic compounds found in the daily consumption of foods (Vitali *et al.,* 2023). A 2022 study quantified plastic particles as small as 66 nm to 5 μm in two brands of bottled water (Huang *et al.,* 2022) which implies the contamination of degraded micro and nano-sized plastic particles and potential intake via oral ingestion. The routes of nanoplastic exposure are illustrated in Figure 1.

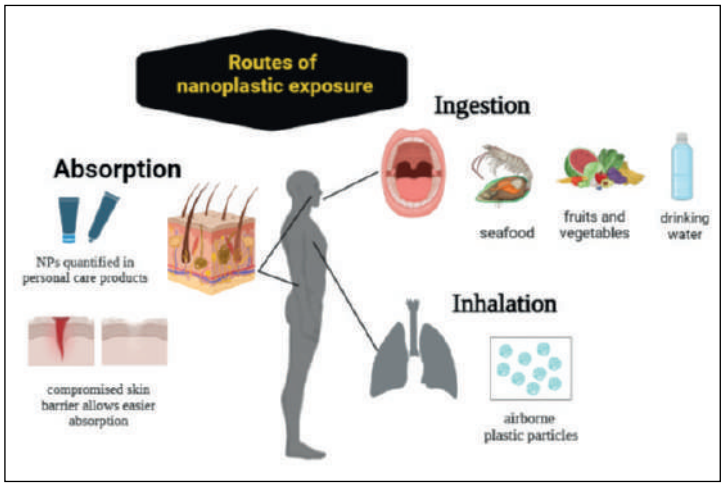

Figure 1. Routes of nanoplastic exposure by ingestion, inhalation and absorption

Many health issues in humans including breathing problems and brain damage are theorised to be caused by nanoplastic exposure (Prust and Meijer, 2020; Zhang *et al.,* 2022). Findings such as neural accumulation of nanoplastics in animal subjects, which give rise to neurodevelopmental problems, behavioural changes and movement abnormalities, became baseline evidence for the ability of these substances to cross the blood brain barrier and its high potential of causing neurotoxicity (Sarasamma *et al.,* 2020).

The National Institute of Neurological Disorders and Stroke defines neurotoxicity as an alteration of nervous system activity by neurotoxicants (toxic natural or man-made substances) (NIH, 2023). According to current evidence relating to induced nanoplastic toxicity, there were two main concerns generated. Firstly, whether PS-NPs could cross the blood brain barrier; Secondly, whether PS-NPs is a potential neurotoxicant and the likely mechanisms involved (Figure 2).

Evidence showed that nanoplastics causes may induce toxic effects on neuronal cell lines (Schröter and Ventura, 2022). Therefore, we determined the mechanism of neurotoxicity of polystyrene nanoplastics (PS-NPs) in SH-SY5Y, a human neuroblastoma cell line widely used in neurological studies.

2. Methodology

2.1 Culture of the SH-SY5Y Cell Line

The human neuroblastoma cell line, SH-SY5Y used in this study was purchased from ATCC (USA). Cells were maintained in Dulbecco's Modified Eagle Medium (DMEM) supplemented with 10% Foetal Bovine Serum (FBS) and 1% Penicillin Streptomycin (Pen Strep) (Gibco, Life Technologies, USA) at 5% CO_2 and 37 °C. Cells were seeded into test plates at optimised cell densities for their respective timepoints.

2.2 Polystyrene Nanoplastic Preparation

Polystyrene nanoplastics nanobeads (PS-NPs) were purchased from Thermo Scientific (USA). Four sizes of PS-NPs were used in this study, namely 20 nm, 40 nm, 50 nm (fluorescent-labelled) and 100 nm. The PS-NPs were already manufactured to their respective nano sizes, with a fixed concentration of 1% solids for every 15 mL bottle. To prepare working concentrations, each of the PS-NP stock was diluted with low serum medium (1% FBS, 1% PenStrep and DMEM) using 5x serial dilution technique from 0.2% PS-NPs concentration. The 7 concentrations used were 0.2%, 0.04%, 0.008%, 0.0016%, 0.00032%, 0.000064%,

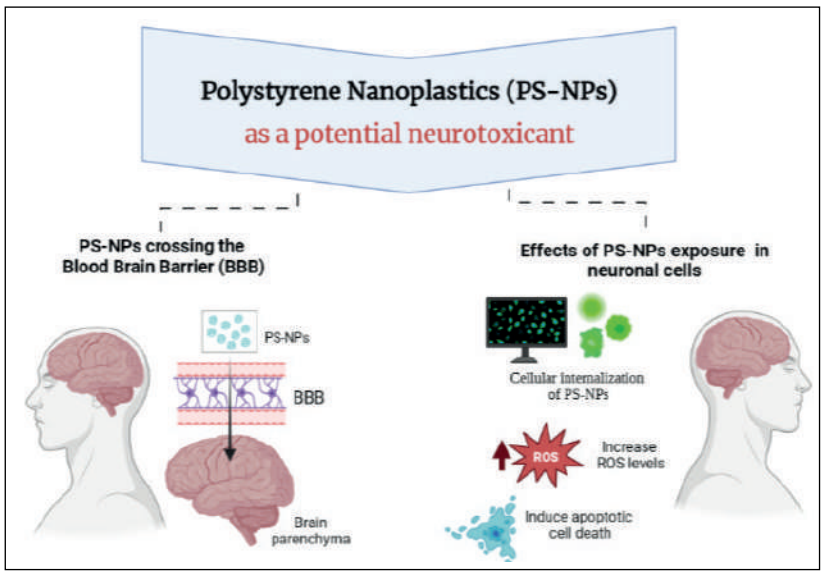

Figure 2. Concerns of PS-NPs as a potential neurotoxicant

0.0000128%. A negative control was also prepared with only SH-SY5Y cells with no treatment of PS-NPs. The concentrations tested were similarly prepared for all four sizes of PS-NPs used in this study.

2.3 Cytotoxicity Assessment with MTT Assay

SH-SY5Y cells were seeded in transparent 96 well plates, at different cell densities optimized for the 3 timepoints used. They were 3.3 x 10^5 cells/well (24 h), 3.0 x 10^5 cells/well (48 h) and 2.8 x 10^5 cells/well (72 h). After treatment of different concentration of PS-NPs for their respective timepoints, MTT (5 mg/mL) was added and was left to incubate for 4 hours in the incubator (5% CO_2 and 37 °C). Then, absorbance reading was taken using a microplate reader (Tecan Infinite 200 Pro, Switzerland) at absorbance value of 570 nm and reference value of 630 nm. From the readings, cell viability in percentage (%) was obtained. The sets of different PSNP sizes (20 nm, 40 nm, 100 nm) were carried out in triplicates and the average cell viability (%) was calculated. When all the sets were completed, a cell viability curve was plotted to extract IC_{50} for each set to determine the most toxic size of PS-NPs. That size and IC_{50} concentration will be used to proceed with the following assays.

2.4 Immunofluorescence Imaging (Engulfment of PS-NPs)

SH-SY5Y cells were seeded in transparent 6 well plates at a cell density of 5.0 x 10^5 cells/well optimised to 24 h timepoint. They were treated with 50 nm fluorescent dyed PS-NPs at IC_{50}, 0.0835% (The IC_{50} of 50 nm PS-NPs was procured from MTT cytotoxicity assay conducted previously). The fluorescent dye type was Firefli™ Fluorescent Green and can be observed at 468/508 nm. After 24 h incubation of seeded cells with PS-NPs treatment, the plate was observed under a fluorescence microscope at 200 x and 400 x magnification.

2.5 ROS Levels with DCFH-DA Assay

SH-SY5Y cells were seeded in black 96 well plates, at different cell densities optimised for the 3 timepoints used. They were 3.3 x 105 cells/well (24 h), 3.0 x 10^5 cells/well (48 h) and 2.8 x 10^5 cells/well (72 h). Then the seeded cells were treated with 20 nm PS-NPs and IC_{50} of that set (0.0055%). DCFH-DA (10 µM) reagent was added in the dark and let incubate for 30 minutes at 37 °C. ROS levels were measured using a microplate reader (Tecan Infinite 200 Pro, Switzerland) at 480 nm excitation and 525 nm emission. The sets were done in triplicates and average ROS levels were calculated.

2.6 Nuclear Fragmentation with Hoechst 33258 Staining

SH-SY5Y cells were seeded in transparent 6 well plates, at different cell densities optimised for the 3 timepoints used. They were 5.0 x 10^5 cells/well (24 h), 4.5 x 10^5 cells/well (48 h) and 4.25 x 10^5 cells/well (72 h). Following treatment (20 nm PS-NPs, IC_{50} = 0.0055%, 24 h, 48 h, 72 h), Hoechst 33258 (10 mg/mL) was added, and the plate was viewed with an inverted microscope (Nikon Ti-U Inverted Microscope, Japan) at 400 x magnification.

2.7 Quantifying Apoptotic Cells with Flow Cytometry

SH-SY5Y cells were seeded in transparent 6 well plates at the cell density of 5.0 x 10^5 cells/well (24 h). Cell seeding was also carried out using additional 2 x 6 cm petri dishes for compensation. Following treatment (20 nm PS-NPs, IC_{50} = 0.0055%, 24 h); cell harvesting was conducted and FITC Annexin V apoptosis detection kit (BD Pharmingen™, USA) was utilised. The detection kit consisted of FITC Annexin V (5 µL used per test), Propidium Iodide Staining Solution (5 µL used per test) and Annexin V Binding Buffer (10 x).

The cells were washed twice with phosphate buffer solution (PBS) and resuspended with the binding buffer at 1x working solution. In a 5 mL culture tube, 5 µL of FITC Annexin V and 5 µL of Propidium Iodide were added to 100 µL of the mixture of binding buffer and washed cells. The reagents were added in a dark room due to their photosensitive nature. After an incubation

period of 15 minutes at room temperature (25 °C) in the dark, 400 µL of the remaining 1x binding buffer was added to each of the 5 mL tubes. Then using flow cytometry, the gated percentage of apoptotic cells was determined. The flow cytometer utilised was the BD FACSCaliburTM (BD Biosciences, USA) and software used was BD CellQuestTM Pro (BD Biosciences, USA).

2.8 Statistical analysis

To measure the differences of means between groups, Student's independent t-test on Microsoft Excel (Microsoft Office Professional Plus ver. 2016) was used. Results were presented as mean ± SD and a p value of less than 0.05 was considered significant.

3. Results and Discussion

3.1 PS-NP Engulfment by SH-SY5Y Cells

The engulfment of PS-NPs into SH-SY5Y cells was verified by fluorescence microscopy using the FITC function of an inverted fluorescence microscope. Microscopic images were captured at 200 x magnification (Figure 3) and 400 x magnification (Figure 4). Upon observation, it appeared that the 50 nm fluorescence labelled PS-NPs were engulfed by the cells due to their fixation on areas of adherent cells rather than being scattered in other areas of the well plate. A control without PS-NPs treatment (Figure 3A, Figure 4A) was prepared to ensure no fluorescence was emitted by the cells or any substances in the cell medium. The choice of 50 nm PS-NPs in this study is to maintain consistency with concurrent studies conducted by the authors' research team, which had utilised 50 nm for toxicity assays of NPs in cell lines of other tissue origins, for example, gut, lung, skin, and retina. Secondly, a published in vivo study has demonstrated that 50 nm NPs can accumulate in the brain, passing through the blood brain barrier (Shan *et al.,* 2022).

The uptake of nanoplastics had been suggested to be through three methods, passive targeting, active targeting or cell death. Under the normal physiological state, nanoplastics are usually prevented from passively crossing the cell membrane, unless they are smaller than the surface pores which allows bioaccumulation (Lee *et al.,* 2019). Active targeting of nanoplastics is complex involving corona formation and surface modification which facilitates the internalisation of nanoparticles into the cell (Kihara *et al.,* 2019; Baimanoy *et al.,* 2019). Nanoplastics were also shown to induce alteration in structure and dynamics of the cell membrane, resulting in the loss of functionality and death of the cell (Hollóczki *et al.,* 2020). The internalisation of nanoplastics had also been recorded in human lung and intestinal cell lines (Zhang *et al.,* 2022). Use of scanning electron microscope (SEM) or transmission electron microscope (TEM) may further determine the areas of accumulation of PS-NPs for SH-SY5Y cells and study the mechanism of internalisation.

Based on nanoparticle studies, the authors postulate that over-confluence would compromise engulfment due to reduced cell surface area for passive diffusion and endocytosis (Drasler *et al.,* 2017; Oh & Park, 2014). Furthermore, as PS-NPs form protein-coronas and aggregate on cell surfaces prior to endocytosis (Gopinath *et al.,* 2021), the overcrowding of cells would reduce the inclination for aggregation to take place. In small-intestine cells, it was revealed that cellular uptake of NPs is a growth phase-dependent process (Binder *et al.,* 2023), which suggests that it is crucial to maintain cells at the exponential growth phase for NP uptake experiments which corresponds to 50 - 60% confluence.

3.2 PS-NPs Induced Cytotoxicity in SH-SY5Y Cells

To verify the PS-NPs induced cytotoxicity on SH-SY5Y, MTT assay was utilised. Two variables tested were the different sizes and concentrations of PS-NPs. It is found that with increased concentration, there was a decrease in cell viability and the most cytotoxic effect was inflicted by PS-NPs of the smallest size.

3.2.1 Increased PS-NP Concentration Reduces Cell Viability

Cell viability of SH-SY5Y cells reduced when exposed to increasing concentration of PS-NPs. This is especially observed to be statistically significant from 0.008% to 0.2% PS-NPs in 100 nm and 40 nm (Figure 5A, B), while a sharp drop in cell viability can be seen even from 0.00016% for 20 nm PS-NPs (Figure 5C). Incidentally, there were two outliers showing an increased cell viability trend of 40 nm PS-NPs exposure at 24 h around the lower concentrations, and 20 nm at 72 h around the higher PS-NPs concentration exposure.

Studies on nanoplastic toxicity had explored the possibility of NPs concentration to be a significant factor that affects cell viability. Based on these findings, there was a statistically significant decrease in cell viability with increasing concentration of PS-NPs (Figure 5). This trend was also seen in past studies working with PS-NPs on different human cell lines such as HTR8/SVneo trophoblast cells, A549 lung cells, and HepG2 liver cells (Hu *et al.,* 2022; Shi *et al.,* 2022; He *et al.,* 2020). Nonetheless, a limitation for this deduction is that the concentrations of PS-NP treatment used in most nanoplastic toxicity studies were allegedly much higher than the actual number of PS-NPs quantified in human

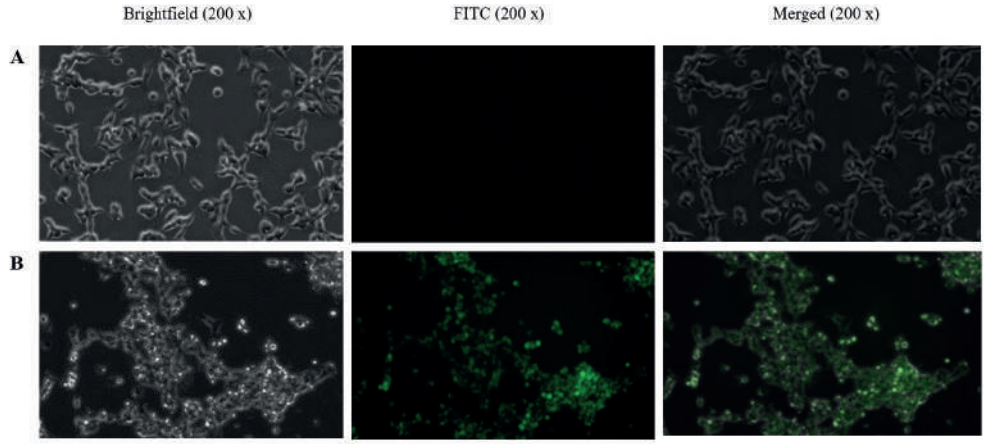

Row A shows the control (SH-SY5Y cells without PS-NPs treatment) at 24 h timepoint; Row B shows the results for SH-SY5Y cells exposed to IC_{50} concentration of 50 nm fluorescent PS-NPs treatment

Figure 3. PS-NP engulfment visualised at 200 x magnification

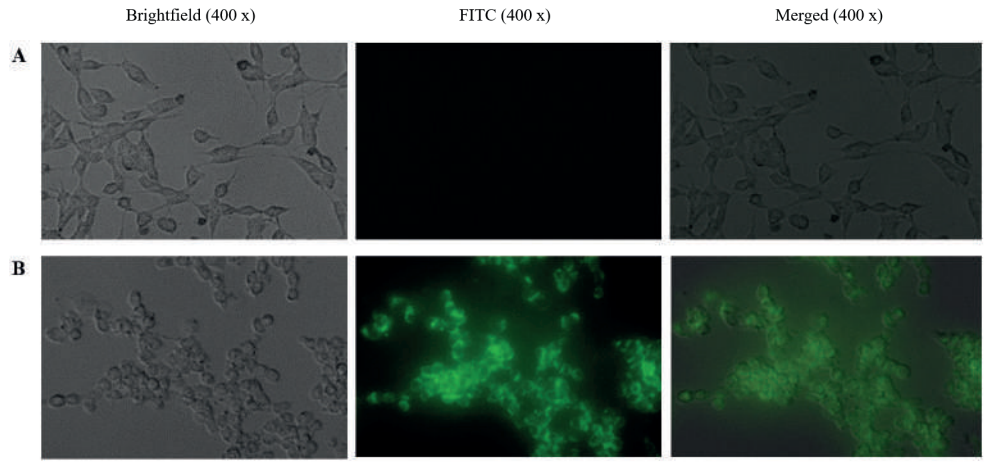

Row A (control) and row B (treated with IC_{50} PS-NPs) at 24 h timepoint

Figure 4. PS-NP engulfment visualised at 400 x magnification

systems. Despite this, to authors' knowledge, no quantification of NPs in human systems were successfully compiled due to lack of sensitive detection and isolation methods.

Incidentally, an increase in cell viability at certain PS-NPs concentration tested was observed. Similar findings have also been discovered in several studies (Jung *et al.,* 2020) which theorised on cytoprotective mechanism and reactive proliferation towards PS-NPs exposure. At certain levels of PS-NP concentration and after a certain timepoint, there was a decrease in ROS level possibly caused by increased protective antioxidant activity, which could have contributed to the survival of the cells and increase in cell viability (Gopinath *et al.,* 2021).

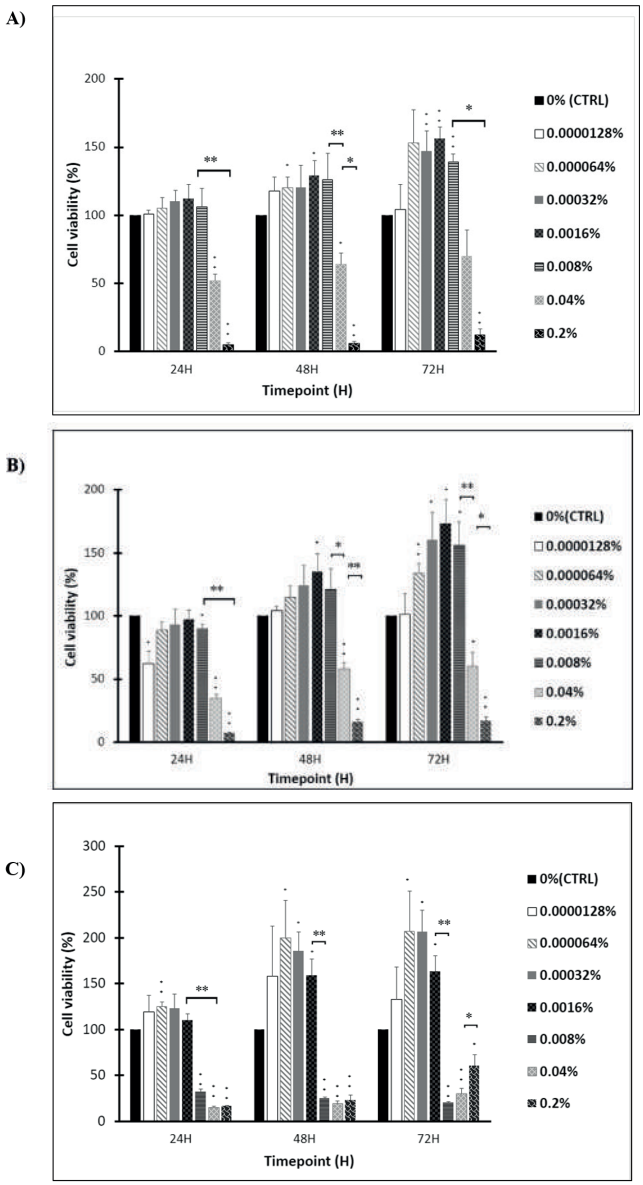

(A) represents cell viability (%) of SH-SY5Y when exposed to 100 nm PS-NPs at 7 concentrations plus a control; (B) 40 nm PS-NPs, and (C) 20 nm PS-NPs
The cell viability was measured over a span of 24 h, 48 h and 72 h timepoints
Statistical significance is shown as *p < 0.05, **p < 0.01. Bar graphs represent the cell viability in mean (of triplicates) ± SD

Figure 5. Effect of PS-NP concentration on cell viability of SH-SY5Y

One of the novelties of this study is the utilisation of a wide range of concentrations from 0.2% (2000 µg/mL) to 0.0000126% (0.126 µg/mL). As mentioned in section 2.4.1, the amount of polystyrene found in human blood can be as high as 4.8 µg/mL. This falls in between the tested concentrations of 0.00032% (3.2 µg/mL) and 0.0016% (16 µg/mL). However, the trend of cytotoxicity for this range remains inconclusive as no statistically significant differences were determined. Therefore, further research could be carried out using a focused dilution factor around this range to test for significant trends in cytotoxicity more accurately.

3.2.2 Decrease in PS-NP Size Reduces Cell Viability

The inhibitory concentration, IC_{50} was adopted to determine the most toxic size for PS-NPs. Based on the cell viability curves (Figure 6B, D, F), the smallest size of PS-NPs had the most toxic effect, where only 0.0055% concentration of 20 nm PS-NPs was needed to reduce cell viability of SH-SY5Y cells by half; compared to 40 nm and 100 nm PS-NPs. The authors found variations in the IC_{50} for 20 nm across all time points, however, the difference in values were well below 4 decimal places (almost negligible), thus they appear consistent at 0.0055%.

From the cytotoxicity findings, the smallest size of PS-NPs induced the most toxic effect on the cells. This is in line with the findings by Xu *et al.* (2019) and Shi *et al.* in their study with human cell line A549 lung epithelial cells, where smaller PS-NPs showed greater internalisation and contributed to gene expression disturbances, increased inflammatory responses, reduced cell viability and apoptotic cell death (Xu *et al.,* 2019; Halimu *et al.,* 2022). It may be deduced that smaller sized particles allowed higher internalisation and bioaccumulation due to their passive transport across the cellular membrane, and increased formation of protein coronas which facilitate engulfment into the cell (refer to 3.1). As internalisation prerequisites induced toxicity, particularly associated with the intrinsic mitochondrial apoptotic mechanism, it may be deduced that smaller nanoplastics inflict greater toxicity to cells and tissues compared to bigger particles. Nonetheless, our findings contradict Lei *et al,* who showed that in Caenorhabditis elegans, 1 µm microplastics (MPs) were more toxic compared to smaller (100 nm) NPs, which implies that toxicity depends on both the size of plastics and host species (Lei *et al.,* 2018).

It is important to note that for this study, nanoplastics were utilised instead of microplastics as hypothethically, their smaller size was considered a major factor affecting cytotoxicity. This is supported by Sharma *et al.* (2022) who reasoned that nanoplastics were more dangerous than microplastics and thus should require more attention in this field of research.

3.3 PS-NPs Raises ROS Levels in SH-SY5Y Cells

Intracellular ROS was measured using the DCFH-DA assay whereby the intensity of fluorescence detected was proportional to the level of cellular ROS. In all three timepoints, the ROS levels showed an increasing trend compared to the negative (untreated) control (Figure 7) although not statistically significant and thereby inconclusive. However, it has been reported in other studies that increased ROS levels were consistently observed, such as an induced ROS production seen in HaCaT (human keratinocyte) cell line (Gopinath *et al.,* 2021) and similarly using HeLa (human epithelial) and T98G (neuronal) cell lines (Schirinzi et al., 2017). It is important to discuss on the impact of increased oxidative stress, as numerous articles have postulated significant linkages between oxidative damage with neurodevelopmental disorders and neurodegenerative diseases.

While natural product cytotoxicity assays involve the use of positive controls (usually hydrogen peroxide for ROS and cytotoxic drugs/heat treatment for apoptosis), as this is an *in vitro* toxicity study based on nanoplastic uptake, therefore an authentic positive control to trigger cell death due to the

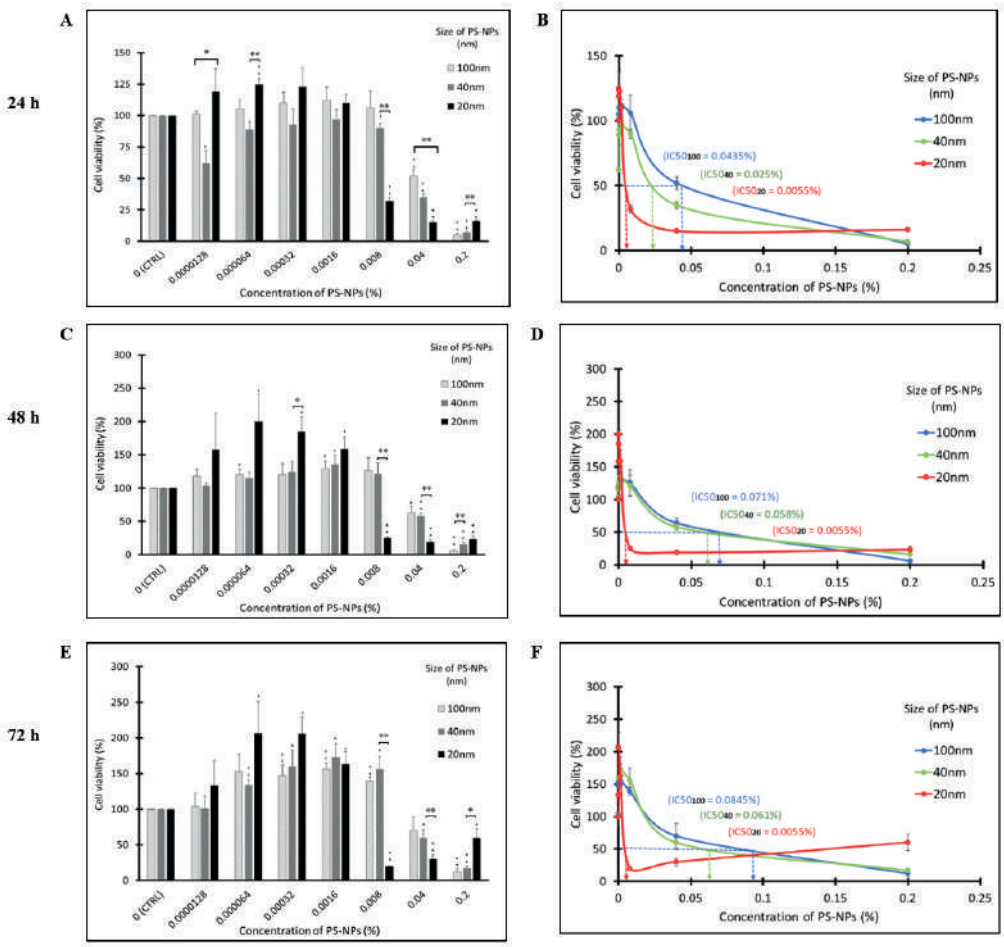

A, C, E shows the results of cell viability for 3 different sizes of PS-NPs (20 nm, 40 nm, 100 nm) for the 24 h, 48 h and 72 h timepoint respectively at 7 different concentrations plus a control Similarly, the adjacent curve B, D, F displays the cell viability but is plotted against a fixed ascending concentration value, which allows interpolation of IC_{50} at 50% cell viability Statistical significance is shown as *p<0.05, **p<0.01

Figure 6. Effect of PS-NP size on cell viability of SH-SY5Y

particle engulfment has yet to be established. On this basis, we rationalised that a negative (untreated) control would suffice to account for any unknown variables that may be present in the experiment. Furthermore, we referred to several *in vitro* toxicity studies published on polystyrene NPs demonstrated similar experimental designs without positive controls (He *et al.,* 2020; Wan *et al.,* 2024; Yan *et al.,* 2023).

ROS is physiologically produced as a natural byproduct of cellular metabolism in the mitochondria. Low to moderate levels of ROS are vital for the normal function of systems such as inflammatory reactions, immune responses, active synaptic plasticity and normal brain functions. However, when there is an excess in ROS production, an imbalance between the free radicals and antioxidants occurs, leading to an adverse phenomenon known as oxidative stress. Oxidative stress causes cell damage, producing noxious oxidative modifications to the cell organelles, particularly targeting the mitochondria (Cenini *et al.,* 2019). Mitochondrial damage itself will generate ROS, which further contributes to oxidative stress and triggers a cascade of events, which can result in apoptotic cell death (discussed in 3.4).

Notably, the brain is a particularly vulnerable organ to oxidative damage due to high oxygen demand, high production of

ROS (critical for redox signalling pathways to regulate synaptic plasticity) and lower content of antioxidants compared to other organs (Cobley *et al.,* 2018). Other factors such as aging and diseased conditions could impair antioxidant productions, failing to inhibit increased ROS levels in the brain. Oxidative stress has been shown to contribute to the pathophysiology of increasingly common neurodegenerative diseases such as Alzheimer's disease (AD) and Parkinson's disease (PD) (Cassidy *et al.,* 2020; Chang and Chen, 2020). Evidence also suggested that oxidative stress relate to neurodevelopmental disorders such as autism spectrum and attention deficit/hyperactivity disorders (ADHD) (Usui *et al.,* 2023; Corona *et al.,* 2020). Nonetheless, the discovery of nanoplastics inducing a rise of ROS levels should be further investigated, as this possible link could be important to explain the rapidly increasing number of neurological cases recorded today.

3.4 PS-NPs Induces Apoptotic Cell Death in SH-SY5Y Cells

In this study, two methods were employed to investigate whether PS-NPs induced apoptotic cell death in SH-SY5Y cells. For a qualitative measure, Hoechst 33258 is used to stain the nuclear material of the cells allowing visualisation and image capture of nuclear changes of exposed cells to PS-NPs compared to the control (Figure 8). For quantitative measure, the FITC Annexin V/ Propidium Iodide Apoptosis Detection Kit was used along with flow cytometry allowing the gated percentage of cells to be generated in each of the respective quadrants (Figure 9). This study selected 20 nm PS-NPs to study the cytotoxic mechanism of PS-NPs as cellular toxicity was apparent across all time points. The 24 h timepoint was preferred for flow cytometry (apoptosis) based on the rationale that early apoptotic changes may be observed before extensive cell death which could confound the data. The selected NP size was 20 nm for ROS (oxidative stress) and flow cytometry (apoptosis) assays as it showed the lowest IC_{50} based on MTT assay findings. Since our focus was to explore the mechanism of cytotoxicity, we postulated that 20 nm would yield the most significant changes compared to 40 nm and 100 nm sized PS-NPs.

3.4.1 Hoechst 33258 Staining

Images captured at 400 x magnification allow visualisation of cell nuclei stained with Hoechst 33258 under DAPI setting. The results showed distinctive DNA fragmentations (Figure 8) which is the hallmark for apoptosis in 24 h, 48 h and 72 h timepoint for treated cells.

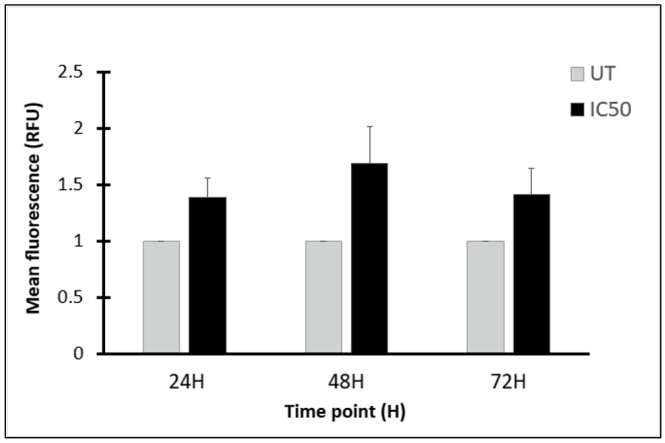

The column displays the average ROS levels of exposed SH-SY5Y cells to 20 nm PS-NPs at IC_{50} (0.0055%) concentration at 24 h, 48 h and 72 h presented as mean ± SD

Figure 7. Effect of 20 nm PS-NPs on levels of intracellular ROS of SH-SY5Y cells

3.4.2 Annexin V/ Propidium Iodide Flow Cytometry

Flow cytometry showed an increase in gated percentage of cells within the upper and lower right quadrant (late and early apoptotic phases respectively) for treated cells, while the control (untreated cells) had most of the gated percentage of cells within the lower left quadrant (viable). This quantified a greater number of viable cells for the untreated group, and greater number of apoptotic cells in PS-NPs treated group.

A popular theory for the mechanism of cell death induced by PS-NPs is by mediation of the mitochondrial apoptotic pathway, but this study proved that apoptosis was induced in PS-NP exposed neuronal cells. The two apoptotic tests employed in this study revealed a positive finding for apoptosis, where nuclear DNA fragmentation (a hallmark of apoptosis) can be observed using Hoechst 33258 staining and an increased percentage of 18.18% apoptotic cells were quantified using flow cytometry. The mitochondrial apoptotic pathway was investigated in the CaCo-2 (colorectal adenocarcinoma) cell line, where vital apoptotic mediator proteins such as Caspase 9 and Caspase 3 were detected by Western Blotting in exposed cells to PS-NPs (Yan *et al.,* 2023).

Studies indicate that oxidative stress is a major factor inducing mitochondrial mediated apoptosis. Once triggered, a cascade of cellular activities involving cytochrome c release, activation of Caspase 9 and Caspase 3 eventually results in apoptotic cell death (Redza *et al.,* 2016). Notably, the current findings of increased ROS levels by PS-NPs were revealed to be not significant, therefore implying that our results were inconclusive for oxidative stress in SH-SY5Y. Nonetheless, based on findings from the apoptotic assays, the mechanism of cell death in SH-SY5Y strongly favours mitochondrial apoptosis (Figure 10). Although apoptosis is a normal process of programmed cell death, uncontrollable apoptosis could lead to neurodegenerative diseases, disruption of neurotransmitter production and ultimately brain damage, which is detrimental for the normal nervous function of living organisms.

3.5 Remedial theories on NPs as a neurotoxicant

Since nanoplastics are potential neurotoxicants, scientists had begun researching possible remedial means to address these adverse neurotoxic effects. Wang *et al* (2023), in his study involving neurological status of mice, discovered that the brain damage caused by nanoplastic exposure could be reversed if ingestion was halted after some time. This implies that brain damage induced by nanoplastics could be alleviated if the plastic exposure was ceased. This discovery contributes to the movement of ending plastic pollution globally (Yang *et al.,* 2023).

4. Conclusion

In conclusion, this study demonstrated that PS-NPs appeared to be engulfed by SH-SY5Y cells. Compared to the control group, the results also showed a significant concentration-dependent and size-dependent decrease in cell viability of exposed SH-SY5Y cells to PS-NPs. Furthermore, it was also postulated that PS-NPs increased intracellular ROS levels in SH-SY5Y cells, although findings were not statistically significant. Lastly, this study showed an induction of apoptosis by PS-NPs on SH-SY5Y both qualitatively (Hoechst staining) and quantitatively (flow cytometry). In essence, PS-NPs may induce cytotoxicity via apoptosis in a neuronal cell line.

Further investigations on the cytotoxic signalling pathways should utilise more advanced imaging such as scanning electron microscope (SEM) or transmission electron microscope (TEM). Tracking of secondary messengers of the apoptotic pathway can also be done to gather evidence of nanoplastic-induced apoptosis at a molecular level.

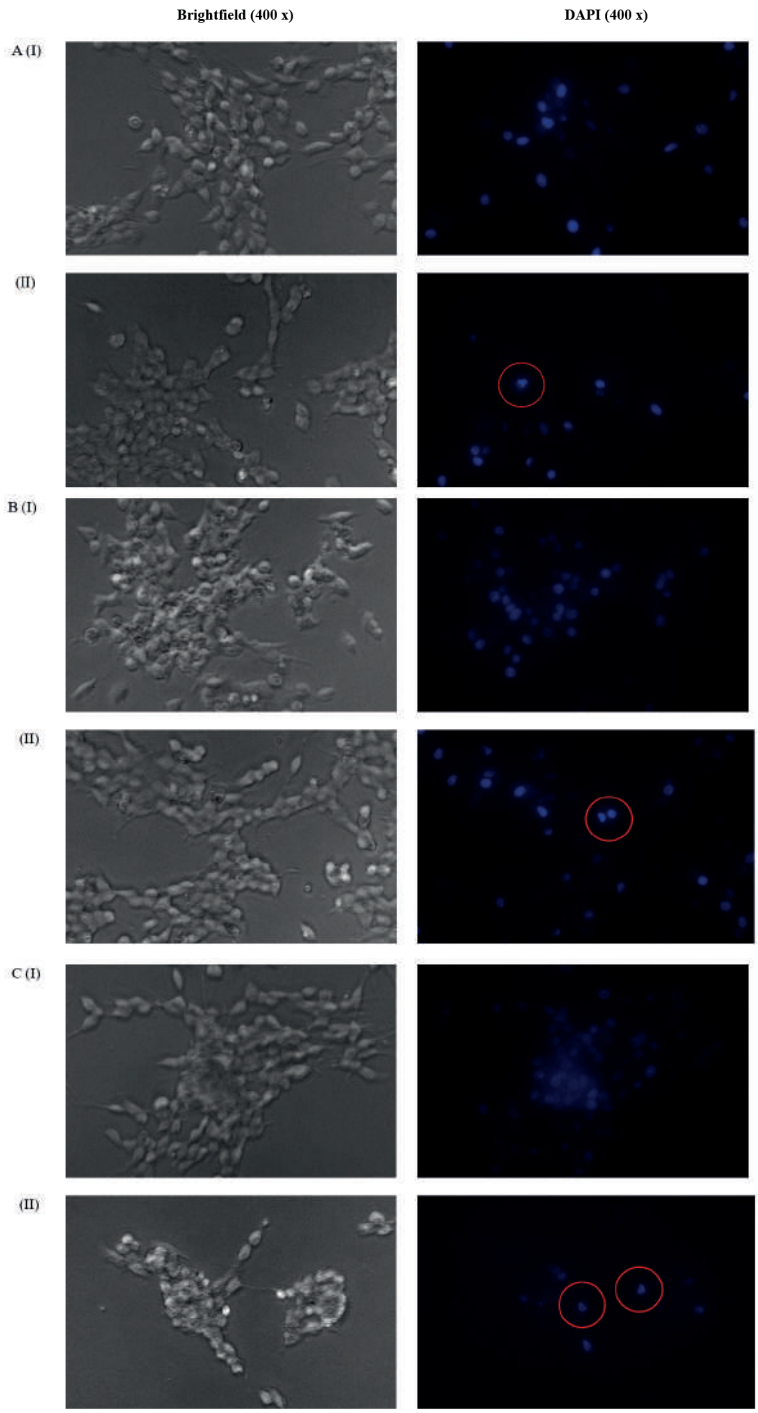

Micrograph A(I) and (II) shows the brightfield and DAPI images for the Control and Treated (IC_{50}) cells respectively for the 24 h timepoint
In a similar arrangement, B(I) and (II) are the results for the 48 h timepoint, and C(I) and (II) depicts results for 72 h timepoint
The cells highlighted with a red circle illustrated signs of apoptosis, where nuclear fragmentation (nuclear material appears condensed and separated, no longer maintaining
an intact circular shape) can be observed

Figure 8. Apoptotic features in SH-SY5Y cells exposed to 20 nm PS-NPs

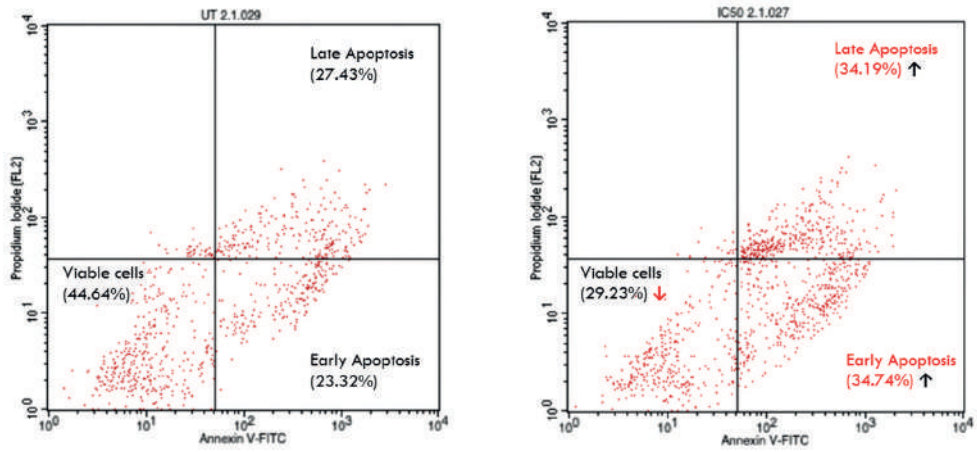

The left scatter plot shows quantification for control (untreated), while the right scatter plot shows quantification for treated cells with IC_{50} concentration (0.0055%)

Figure 9. Effect of exposure to 20 nm PS-NPs on apoptosis in SH-SY5Y cells for 24 h timepoint

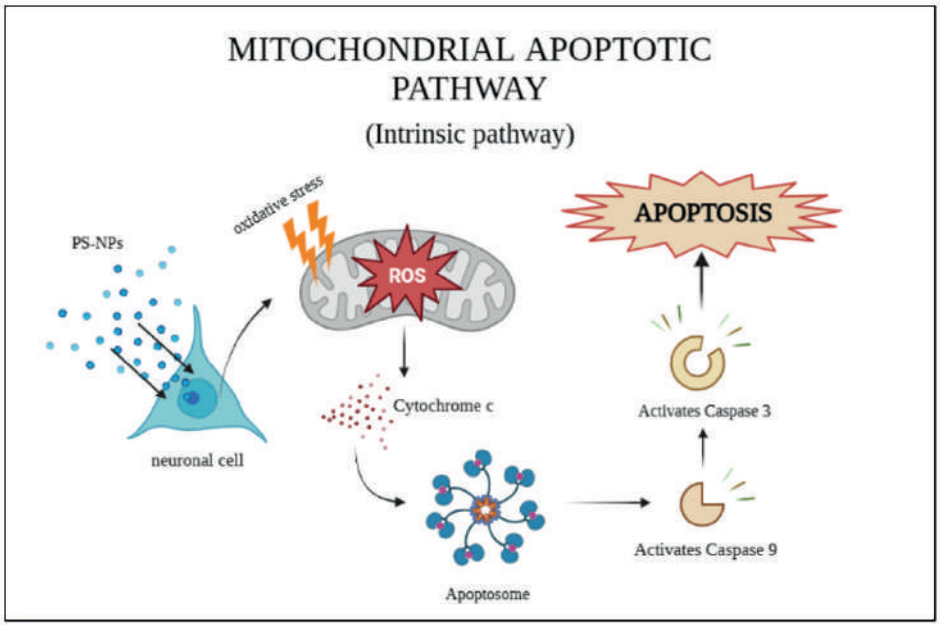

PS-NPs induce oxidative stress in a neuronal cell, prompting increased production of mitochondrial ROS

This initiates the release of cytochrome c into the cytoplasm of the cell, which forms numerous apoptosomes (complex protein structures made up of four components, cytochrome c, adenosine triphosphate (ATP), apoptosis-activating factor (Apaf-1) and procaspase-9)

The apoptosome activates Caspase-9, which in turn activates Caspase-3. Once this terminal caspase is activated, it responds by executing the proteolytic processes of apoptosis

Figure 10. Oxidative stress induce mitochondrial apoptotic pathway in a neuronal cell

Acknowledgement

The study was supported by the IMU University Bachelor of Medical Sciences (BMedSc) programme grant with ethical approval (Project ID: BMS I-2022 (02)). The authors are grateful for the provision of laboratory space facilities and support, as well as Ms. Dorea Soong Shi Hui for sharing her expertise and experience on working with SH-SY5Y cells and laboratory assays.

References

Abbasi S. Routes of human exposure to micro(nano)plastics. Current Opinion in Toxicology 2021; 27: 41–46. Available from: https://doi.org/10.1016/j.cotox.2021.08.004

Baimanov D, Cai R & Chen C. Understanding the Chemical Nature of Nanoparticle-Protein Interactions. Bioconjugate Chemistry 2019; 30(7): 1923–1937. Available from: https://doi.org/10.1021/acs.bioconjchem.9b00348

Binder ARD, Mussack V, Kirchner B & Pfaffl MW. Uptake and effects of polystyrene nanoplastics in comparison to non-plastic silica nanoparticles on small intestine cells (IPEC-J2). Ecotoxicology and Environmental Safety 2023; 262: 115147. Available from: https://doi.org/10.1016/J.ECOENV.2023.115147

Cassidy L, Fernandez F, Johnson JB, Naiker M, Owoola AG & Broszczak DA. Oxidative stress in alzheimer's disease: A review on emergent natural polyphenolic therapeutics. Complementary Therapies in Medicine 2020; 49: 102294. Available from: https://doi.org/10.1016/j.ctim.2019.102294

Cenini G, Lloret A, & Cascella R. Oxidative Stress in Neurodegenerative Diseases: From a Mitochondrial Point of View. Oxidative Medicine and Cellular Longevity 2019; e2105607. Available from: https://doi.org/10.1155/2019/2105607

Chang K.H, & Chen CM. The Role of Oxidative Stress in Parkinson's Disease. Antioxidants 2020; 9(7), Article 7. Available from: https://doi.org/10.3390/antiox9070597

Cobley JN, Fiorello ML & Bailey DM. 13 reasons why the brain is susceptible to oxidative stress. Redox Biology 2018; 15: 490–503. Available from: https://doi.org/10.1016/j.redox.2018.01.008

Corona JC. Role of Oxidative Stress and Neuroinflammation in Attention-Deficit/Hyperactivity Disorder. Antioxidants 2020; 9(11), Article 11. Available from: https://doi.org/10.3390/antiox9111039

Drasler B, Vanhecke D, Rodriguez-Lorenzo L, Petri-Fink A & Rothen-Rutishauser B. Quantifying Nanoparticle Cellular Uptake: Which Method is Best? Nanomedicine 2017; 12(10): 1095–1099. Available from: https://doi.org/10.2217/NNM-2017-0071

Geng Y, Zhang Z, Zhou W, Shao X, Li Z & Zhou Y. Individual Exposure to Microplastics through the Inhalation Route: Comparison of Microplastics in Inhaled Indoor Aerosol and Exhaled Breath Air. Environmental Science & Technology Letters 2023; 10(6): 464–470. Available from: https://doi.org/10.1021/acs.estlett.3c00147

Gigault J, Halle A. ter, Baudrimont M, Pascal PY, Gauffre F, Phi TL, El Hadri H, Grassl B & Reynaud S. Current opinion: What is a nanoplastic? Environmental Pollution 2018; 235: 1030–1034. Available from: https://doi.org/10.1016/j.envpol.2018.01.024

Gopinath PM, Twayana K.S, Ravanan P, John Thomas, Mukherjee A, Jenkins DF & Chandrasekaran N. Prospects on the nano-plastic particles internalization and induction of cellular response in human keratinocytes. Particle and Fibre Toxicology 2021; 18(1): 35. Available from: https://doi.org/10.1186/s12989-021-00428-9

Halimu G, Zhang Q, Liu L, Zhang Z, Wang X, Gu W, Zhang B, Dai Y, Zhang H, Zhang C & Xu M. Toxic effects of nanoplastics with different sizes and surface charges on epithelial-to-mesenchymal transition in A549 cells and the potential toxicological mechanism. Journal of Hazardous Materials 2022; 430: 128485. Available from: https://doi.org/10.1016/j.jhazmat.2022.128485

He Y, Li J, Chen J, Miao X, Li G, He Q, Xu H, Li H & Wei Y. Cytotoxic effects of polystyrene nanoplastics with different surface functionalization on human HepG2 cells. Science of The Total Environment 2020; 723: 138180. Available from: https://doi.org/10.1016/j.scitotenv.2020.138180

Hollóczki O & Gehrke S. Can Nanoplastics Alter Cell Membranes? ChemPhysChem 2020; 21(1): 9–12. Available from: https://doi.org/10.1002/cphc.201900481

Hu J, Zhu Y, Zhang J, Xu Y, Wu J, Zeng W, Lin Y & Liu X. The potential toxicity of polystyrene nanoplastics to human trophoblasts in vitro. Environmental Pollution 2022; 311: 119924. Available from: https://doi.org/10.1016/j.envpol.2022.119924

Huang Y, Wong KK., Li W, Zhao H, Wang T, Stanescu S, Boult S, van Dongen B, Mativenga P & Li L. Characteristics of nano-plastics in bottled drinking water. Journal of Hazardous Materials 2022; 424: 127404. Available from: https://doi.org/10.1016/j.jhazmat.2021.127404

Joseph AD. Styrofoam Facts—Why You May Want To Bring Your Own Cup. SEJ. 2019. Available from: https://www.sej.org/publications/backgrounders/styrofoam-facts-why-you-may-want-bring-your-own-cup

Jung BK, Ha SW, Park SH, Bae JS, Choi J & Ryu KY. Neurotoxic potential of polystyrene nanoplastics in primary cells originating from mouse brain. NeuroToxicology 2020; 81: 189–196. Available from: https://doi.org/10.1016/j.neuro.2020.10.008

Kihara S, van der Heijden NJ, Seal CK, Mata JP, Whitten AE, Köper I & McGillivray DJ. Soft and Hard Interactions between Polystyrene Nanoplastics and Human Serum Albumin Protein Corona. Bioconjugate Chemistry 2019; 30(4): 1067–1076. Available from: https://doi.org/10.1021/acs.bioconjchem.9b00015

Lai H, Liu X & Qu M. Nanoplastics and Human Health: Hazard Identification and Biointerface. Nanomaterials 2022; 12(8): 1298. Available from: https://doi.org/10.3390/nano12081298

Lambert S & Wagner M. Characterisation of nanoplastics during the degradation of polystyrene. Chemosphere 2016; 145: 265–268. Available from: https://doi.org/10.1016/j.chemosphere.2015.11.078

Lee WS, Cho HJ, Kim E, Huh YH, Kim HJ, Kim B, Kang T, Lee JS & Jeong J. Bioaccumulation of polystyrene nanoplastics and their effect on the toxicity of Au ions in zebrafish embryos. Nanoscale 2019; 11(7): 3173–3185. Available from: https://doi.org/10.1039/C8NR09321K

Lei L, Liu M, Song Y, Lu S, Hu J, Cao C, Xie B, Shi H & He D. Polystyrene (nano)microplastics cause size-dependent neurotoxicity, oxidative damage and other adverse effects in Caenorhabditis elegans. Environmental Science: Nano 2018; 5(8): 2009–2020. Available from: https://doi.org/10.1039/C8EN00412A

Leslie HA, van Velzen MJM, Brandsma SH, Vethaak AD, Garcia-Vallejo JJ & Lamoree MH. Discovery and quantification of plastic particle pollution in human blood. Environment International 2022; 163: 107199. Available from: https://doi.org/10.1016/j.envint.2022.107199

Lett Z, Hall A, Skidmore S & Alves NJ. Environmental microplastic and nanoplastic: Exposure routes and effects on coagulation and the cardiovascular system. Environmental Pollution 2021; 291: 118190. Available from: https://doi.org/10.1016/j.envpol.2021.118190

Mason L. Revealed: Plastic ingestion by people could be equating to a credit card a week. (n.d.). 2023 Available from: https://wwf.panda.org/wwf_news/?348337/Revealed-plastic-ingestion-by-people-could-be-equating-to-a-credit-card-a-week

NIH. Neurotoxicity. (n.d.). National Institute of Neurological Disorders and Stroke. 2023. Available from: https://www.ninds.nih.gov/health-information/disorders/neurotoxicity

Oh N & Park JH. Endocytosis and exocytosis of nanoparticles in mammalian cells. International Journal of Nanomedicine 2014; 9(Suppl 1). Available from: 51. https://doi.org/10.2147/IJN.S26592

Pauly JL, Stegmeier SJ, Allaart HA, Cheney RT, Zhang PJ, Mayer AG & Streck RJ. Inhaled cellulosic and plastic fibers found in human lung tissue. Cancer Epidemiology, Biomarkers & Prevention: A Publication of the American Association for Cancer Research, Cosponsored by the American Society of Preventive Oncology 1998; 7(5): 419–428.

Prüst M, Meijer J & Westerink RHS. The plastic brain: Neurotoxicity of micro- and nanoplastics. Particle and Fibre Toxicology 2020; 17(1): 24. Available from: https://doi.org/10.1186/s12989-020-00358-y

Redza-Dutordoir M & Averill-Bates DA. Activation of apoptosis signalling pathways by reactive oxygen species. Biochimica et Biophysica Acta (BBA) - Molecular Cell Research 2016; 1863(12): 2977–2992. Available from: https://doi.org/10.1016/j.bbamcr.2016.09.012

Ritchie H & Roser M. Plastic Pollution. Our World in Data. 2018. Available from: https://ourworldindata.org/plastic-pollution

Sarasamma S, Audira G, Siregar P, Malhotra N, Lai YH, Liang ST, Chen JR, Chen KHC & Hsiao CD. Nanoplastics Cause Neurobehavioral Impairments, Reproductive and Oxidative Damages, and Biomarker Responses in Zebrafish: Throwing up Alarms of Wide Spread Health Risk of Exposure. International Journal of Molecular Sciences 2020; 21(4): 1410. Available from: https://doi.org/10.3390/ijms21041410

Savelli H. Fashion's tiny hidden secret. UNEP. 2019. Available from: http://www.unep.org/news-and-stories/story/fashions-tiny-hidden-secret

Schirinzi GF, Pérez-Pomeda I, Sanchís J, Rossini C, Farré M & Barceló D. Cytotoxic effects of commonly used nanomaterials and microplastics on cerebral and epithelial human cells. Environmental Research 2017; 159: 579–587. Available from: https://doi.org/10.1016/j.envres.2017.08.043

Schröter L & Ventura N. Nanoplastic Toxicity: Insights and Challenges from Experimental Model Systems. Small 2022; 18(31): 2201680. Available from: https://doi.org/10.1002/smll.202201680

Shan S, Zhang Y, Zhao H, Zeng T & Zhao X. Polystyrene nanoplastics penetrate across the blood-brain barrier and induce activation of microglia in the brain of mice. Chemosphere 2022; 298: 134261. Available from: https://doi.org/10.1016/J.CHEMOSPHERE.2022.134261

Sharma VK, Ma X, Lichtfouse E & Robert D. Nanoplastics are potentially more dangerous than microplastics. Environmental Chemistry Letters. 2022. Available from: https://doi.org/10.1007/s10311-022-01539-1

Shi X, Wang X, Huang R, Tang C, Hu C, Ning P & Wang F. Cytotoxicity and Genotoxicity of Polystyrene Micro- and Nanoplastics with Different Size and Surface Modification in A549 Cells. International Journal of Nanomedicine 2022; 17: 4509–4523. Available from: https://doi.org/10.2147/IJN.S381776

Usui N, Kobayashi H & Shimada S. Neuroinflammation and Oxidative Stress in the Pathogenesis of Autism Spectrum Disorder. International Journal of Molecular Sciences 2023; 24(6), Article 6. Available from: https://doi.org/10.3390/ijms24065487

Vitali C, Peters RJB, Janssen HG & Nielen MWF. Microplastics and nanoplastics in food, water, and beverages; part I. occurrence. TrAC Trends in Analytical Chemistry 2023; 159: 116670. Available from: https://doi.org/10.1016/j.trac.2022.116670

Wan S, Wang X, Chen W, Wang M, Zhao J, Xu Z, Wang R, Mi C, Zheng Z & Zhang, H. Exposure to high dose of polystyrene nanoplastics causes trophoblast cell apoptosis and induces miscarriage. Particle and Fibre Toxicology 2024; 21(1). Available from: https://doi.org/10.1186/S12989-024-00574-W

Windheim J, Colombo L, Battajni NC, Russo L, Cagnotto A, Diomede L, Bigini P, Vismara E, Fiumara F, Gabbrielli S, Gautieri A, Mazzuoli-Weber G, Salmona M & Colnaghi L. Micro- and Nanoplastics' Effects on Protein Folding and Amyloidosis. International Journal of Molecular Sciences 2022; 23(18): 10329. Available from: https://doi.org/10.3390/ijms231810329

Xu M, Halimu G, Zhang Q, Song Y, Fu X, Li Y, Li Y & Zhang, H. Internalization and toxicity: A preliminary study of effects of nanoplastic particles on human lung epithelial cell. Science of The Total Environment 2019; 694: 133794. Available from: https://doi.org/10.1016/j.scitotenv.2019.133794

Yan L, Yu Z, Lin P, Qiu S, He L, Wu Z, Ma L, Gu Y, He L, Dai Z, Zhou C, Hong P & Li C. Polystyrene nanoplastics promote the apoptosis in Caco-2 cells induced by okadaic acid more than microplastics. Ecotoxicology and Environmental Safety 2023; 249: 114375. Available from: https://doi.org/10.1016/j.ecoenv.2022.114375

Yang Q, Dai H, Cheng Y, Wang B, Xu J, Zhang Y, Chen Y, Xu F, Ma Q, Lin F & Wang C. Oral feeding of nanoplastics affects brain function of mice by inducing macrophage IL-1 signal in the intestine. Cell Reports 2023; 42(4): 112346. Available from: https://doi.org/10.1016/j.celrep.2023.112346

Zhang T, Yang SGY, Wan X, Zhu Y, Li J, Yin L, Pu Y & Liang G. Polystyrene Nanoplastics Induce Lung Injury via Activating Oxidative Stress: Molecular Insights from Bioinformatics Analysis. Nanomaterials 2022; 12(19): 3507. Available from: https://doi.org/10.3390/nano12193507

Zhang YX, Wang M, Yang L, Pan K & Miao AJ. Bioaccumulation of differently-sized polystyrene nanoplastics by human lung and intestine cells. Journal of Hazardous Materials 2022; 439: 129585. Available from: https://doi.org/10.1016/j.jhazmat.2022.129585